Submerged-Arc Stainless Steel Strip Cladding

The development of welding products for surfacing with a Type 316L low ferrite stainless steel alloy involves investigation of the transformation of delta ferrite to sigma phase in 316L-LF alloys

BY R. A. DAEMEN AND F. DEPT

Introduction

Stainless steel alloys of the 316L type with a low amount of ferrite find their principal field of application in the chemical industry for manufacturing urea by synthesis. A maximum content of 2% ferrite is allowed in all the specifications. This amount has been specified principally from the experimental data resulting from short duration corrosion tests of the Huey kind (boiling nitric acid) carried out according to ASTM specifications. There seems to exist a good correlation between the behavior of the alloys in the Huey test and in practical use.

In particular, it is considered that service behavior is satisfactory when the average corrosion rate for 5 test periods of 48 hr. does not exceed 5 microns/48 hr. This rate, expressed in terms of thickness reduction, is obtained by using the following formula:

$$R = \frac{P \times 10000}{S \times D}$$

where R = corrosion rate in microns/hr; P = loss of weight in grams per period; S = area of test piece in sq cm; D = density in gr/cu. cm, i.e. 7.9.

It is also necessary that the depth of local selective attack after five 48 hour periods be less than 200 microns. This is determined by microscopic examinations on cross sections of the test specimen.

It should be noted that the above acceptance limits concern the deposited metals and not the base plate, for which the acceptance limits are different. Tests on metals deposited by manual welding have shown that the acceptance limits laid down for the Huey test are met when the ferrite content of the deposited metal is less than 2%. The purpose of our studies of metals deposited by submerged-arc welding was to use the corrosion acceptance limits as deduced from manual electrode deposits and the ferrite limits which had been established as a starting basis for the development of an automatic cladding method which, for the economy it gives in comparison with the use of electrodes for manual welding, is likely to interest the fabricators.

It became clear nevertheless in course of our investigations that the correlation between the corrosion rate and the ferrite content of the alloy may depend upon the welding process used or more principally upon the thermal conditions characterizing such process.

The different stages of development of the 316L low ferrite strip cladding consumables are discussed in Part I below. The results of some metallurgical investigations dealing with the transformation of delta ferrite to sigma phase in 316L and 316L-LF alloys are discussed in Part II; included is a tentative explanation for accelerated corrosion of these alloys in sigmatised condition.*

* Part I was authored by R. A. Daemen, while Dr. F. Dept prepared Part II.

R. A. DAEMEN is Research Engineer, S. A. Soudometal, Brussels, Belgium, and F. DEPT is an Assistant, Dept. of Metallurgy, State University of Ghent, Belgium.

Part I—Development program and Results

Stage 1

In order to establish a starting basis and to direct the subsequent research, we made a preliminary examination of two overlays referred to as ST 1 and ST 2, respectively medium and low in their ferrite contents. Conditions were as follows:

ST 1: deposited in two layers—thickness 8 mm (1st layer made using strip electrode AISI 309L + flux n° 3252; 2nd layer made using strip electrode AISI 308L + flux n° 3253).

ST 2: deposited in two layers—thickness 8 mm (1st layer made using strip electrode 309L + flux 3254; 2nd layer made using strip electrode 308L + flux 3255).

It should be noted that for these and subsequent tests, strip electrodes of 60 x 0.5 mm (2.36 x .020 in.) cross-section, a welding current of 750-800 amps, 27 v, and a travel speed of 17 cm/min (6.2 ipm), and carbon steel base plates 500 x 250 x 30 mm (10 x 5 x 1.18 in.), and an interpass temperature of 100° C.

Chemical Composition and Ferrite Content of the Metal Deposits. The chemical composition of the metal desposit has been determined in the first and second layers of the deposits;

Table 1—Stage 1 Composition and Ferrite Content of Deposits

		Composition, %						Ferrite, %	
Deposit	Layer	C	Mn	Si	Cr	Ni	Mo	Perma-scope	Micro-scope
	1				16.5	13.9	2.65		
ST 1		0.025	1.3	0.76	18.4	12.4	2.0		
	2	0.026	1.3	0.74	18.6	12.3	2.1	6.9–7.9–8.5	7
					17.4	12.7	2.5		
					15.3	13.9	2.80		
ST 2		0.03	1.55	0.76	17.7	14	2.4		
	2	0.028	1.6	0.89	17.8	13.7	2.6	1.4–1.4–0.6	2
					16.8	13.3	2.7		

Table 2—Stage 1 Corrosion Test Results

	Period, 48 hr	Loss in weight, g 1	2	3	4	5	Average loss in weight, g	Surface, sq cm.	Corrosion rate, microns/ 48 hr[a]
	ST 1/1	0.0597	0.0807	0.2032	....	....	0.1145	27.5136	5.3 (4.47)
ST 1	ST 1/2	0.0909	0.0959	0.1014	....	....	0.0961	32.8367	3.7 (4.18)
	ST 1/3	0.0649	0.0322	0.0431	....	....	0.0467	28.9967	2.05(8.60)
	ST 1/4	0.0805	0.0739	0.1012	....	....	0.0852	31.7616	3.4 (5.30)
	ST 2/1	0.1014	0.0850	....	....	....	0.0982	34.5307	3.7 (9.16)
ST 2	ST 2/2	0.1399	0.1749	....	....	....	0.1574	34.5394	5.8 (9.08)
	ST 2/3	0.1507	0.1966	....	....	....	0.1736	33.7499	6.5(13.51)
	ST 2/4	0.1039	0.1241	....	....	....	0.1140	26.6140	5.45(7.85)

[a] The figures within brackets indicate the corrosion rates determined under similar conditions by the "Staatsmijnen" laboratories, over 5 complete corrosion periods.

the samples have been obtained by machining or drilling down to 2 mm in depth from the as-welded plate surface. The ferrite contents of the metal deposits were determined in the second layer of the deposits. The magnetic measurements carried out by means of the Permascope have been confirmed by microscopic observation. The values obtained are given in Table 1.

Metallographic Examination. The examination had two main aims—the verification of the absence of cracks or microcracks in the cross section and on the surface of the overlays after successive planning operations at different depths across the second layer, and the examination of the structural transformations.

No crack or microcrack was detected in either deposit. In the second layer of ST 1 the ferritic phase was transformed into sigma phase, to the extent of 25 to 50% according to position; in the second layer of ST 2, practically all of the ferrite present was changed into sigma phase. It should be noted that we are confronted here with "as-clad" samples which have not undergone any post-weld heat treatment.

Corrosion Tests. Huey corrosion tests in boiling dilute nitric acid were carried out in accordance with ASTM specifications.

Two test coupons of 25 x 50 x 3 mm were taken from the middle of the 2nd layer in each of the deposited metals. The bead width was approximately 50 mm. They were marked ST 1/1–ST 1/2 and ST 2/1–ST 2/2.

Two test coupons were also taken in the overlapping zones of adjacent beads; these contained a heat-affected zone in the direction of their greatest length. They were marked ST 1/3–ST 1/4 and ST 2/3–ST 2/4. All the test coupons were subjected to corrosion in the as-welded condition. All the coupon faces were machined, except those corresponding to the "as-clad" surface, which were deliberately left untouched.

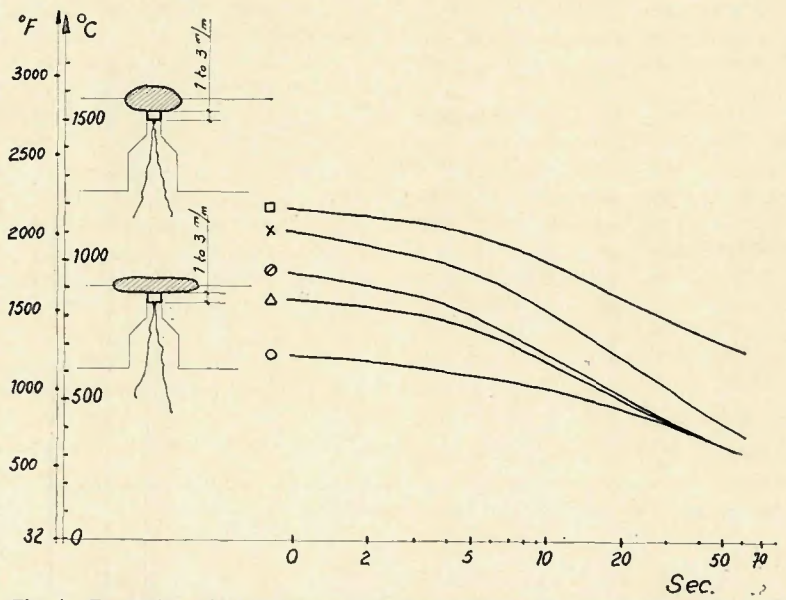

Fig. 1—Examples of weld thermal cycles as recorded under following circumstances: □—strip cladding (strip 60 x 0.5 mm) with thermocouple placed at 3 mm from the fusion line; ×—one electrode submerged-arc welding with thermocouple placed at 1 mm from the fusion line; △—one electron submerged-arc welding with thermocouple placed at 3 mm from the fusion line; ∅—manual arc welding (covered electrode) with thermocouple placed at 1 mm from the fusion line; ○—manual arc welding (covered electrode) with thermocouple placed at 3 mm from the fusion line. 4 mm submerged-arc and covered electrodes

The results obtained are shown in Table 2. In addition, the metallographic examination performed after corrosion have revealed the following depths as resulting from a selective attack: ST 1 after three 48 hr. periods—130 microns; ST 1 after five 48 hr. periods—300 to 330 microns; ST 2 after two 48 hrs. periods—180 microns; ST 2 after five 48 hr. periods—450 to 900 microns.

Conclusions Derived from Stage 1 Experiments.

1. The deposited metals correspond to expectations from the standpoint of chemical composition and metallographic structure.

2. Despite the low ferrite content of the ST 2 deposit and also despite the higher heat input and slower cooling associated with automatic welding, there is no risk of microcracking.[1]

3. Neither the ST 1 type deposit nor the ST 2 type meet the required properties of corrosion resistance. The ST 2 type deposit with 2% ferrite seems to behave worse than the ST 1 type deposit containing on average 7.5% of ferrite.

4. There appears to be no difference in the corrosion behavior between the coupons taken from the middle of the beads and from the adjacent overlapping beads.

5. The metallographic examinations showed an essential structural difference in the 7.5% ferrite alloy, the transformation into a sigma phase only reaches a level of 25 to 50%, whereas in the 2% ferrite alloy, this transformation concerns 100% of the ferrite content. This type of transformation does not occur in similar manual arc deposited metals. It only occurs, during welding, in those metals which are deposited using the strip welding process as a result of slow cooling down of the weld pool.

Figure 1 illustrates the important

Table 3—Stage 2 Coupon Surface Corrosion Test Results

Deposit	Surface condition	48 hr periods—loss in weight, g 1	2	3	4	5	Avg. weight loss, g	Surface, sq cm.	Corrosion rate, micron/ 48 hr	Local attack, microns
ST 1	As-clad	0.1572	0.1695	0.1805	....	....	0.16907	30.3028	7.06	..
	Ground	0.0690	0.0773	0.1200	....	....	0.0888	30.9730	3.62	..
ST 2	As-clad	0.2418	0.2139	0.3256	....	....	0.2604	29.4000	11.2	..
	Ground	0.0925	0.1748	0.3416	....	....	0.2029	29.4500	8.72	..
ST 3	As-Clad	0.2477	0.0847	0.1183	0.1243	0.1621	0.14742	29.1300	6.07	250
	Ground	0.0849	0.0609	0.1180	0.0915	0.1227	0.09562	30.1100	4.02	185

differences between the weld thermal cycles, as recorded in the heat-affected zone at different distances from the fusion line, for manual arc welding, submerged-arc welding with one electrode and submerged-arc strip welding. Especially in the case of the presently considered 2% ferrite alloy (ST 2), it is expected that the sigma phase formation during cladding is responsible for the accelerated corrosion and for the excessive depth of local attack.

Stage 2

Additional Preliminary Investigations. Before starting development of cladding products, it was decided to study the influence of a factor which could have played a role in the corrosion behavior of samples ST 1 and ST 2. This was the condition of the coupon surface.

In consequence, six test coupons were submitted to corrosion: one coupon ST 1—middle of the bead—as-clad surface; one coupon ST 1—middle of the bead—cladding ground; one coupon ST 2—middle of the bead—as-clad; one coupon ST 2—middle of the bead—ground surface; one coupon ST 3—middle of the bead—as-clad; one coupon ST 3—middle of the bead—ground surface.

It should be noted that the ST 3 deposit was of the same kind as ST 2, but with maximum 1% ferrite. It represented a first attempt to improve the corrosion resistance.

The results are given in Table 3. They lead to the following comments:

1. ST 2 compares to ST 1 in the same way as in stage 1, both in the case of the as-clad coupons and of the ground ones.

2. The grinding of the as-clad surface seems to improve corrosion resistance. Yet, it must be pointed out that short duration tests are concerned here and that the observed improvement seems chiefly to be due to the fact that for the ground test pieces, the corrosion rates are lower in the first 2 or 3 forty-eight hour periods. After the second or the third period, it seems that the behavior of the as-clad and ground coupons tend to be similar. This behavior is explained by the presence of a workhardened film resulting from the grinding operation. After the second or third period, this film would be broken through and the beneficial effect would be lost.

3. As for the test specimen ST 3, although not yet entirely satisfactory from the point of view of the corrosion rate and depth of local attack, this is the one which behaves the best. The modification introduced in comparison with ST 2 seems, therefore, to be effective.

Extended Investigations. Four new tests were made, all very low ferrite versions.

1. ST 4—1st layer: strip electrode 309L, flux 3333; 2nd layer: strip electrode 308L, flux 3334.

2. ST 5—1st layer: strip electrode 309L, flux 3338; 2nd layer: strip electrode 308L, flux 3339.

3. ST 6—1st layer: strip electrode 309L, flux 3335; 2nd layer: strip electrode 308L, flux 3337/5.

4. ST 7—1st layer: strip electrode 309L, flux 3336; 2nd layer: strip electrode 308L, flux 3337/6.

The dimensions of the strip, the working conditions and the welding parameters are similar to those employed during the first stage.

Chemical Composition and Ferrite Content of Stage 2 Deposits. The chemical compositions for the first and second layers of deposited metal are given in Table 4. This table also contains permeability data dealing with the ferrite contents of the metal deposits. Since we are dealing with very low ferrite contents, the Permascope method has been abandoned in favor of a more precise determination of the magnetic permeability of the alloys as shown by a Magnetoscope. It works with a magnetic field of about a 1000 Oe intensity. The conversion of the measured magnetic permeabilities into ferrite content is possible using the calibration curve shown in Fig. 2. This correlation curve has been established in our laboratories, on weld deposits, and is based upon metallographic investigations.

Metallographic Examinations. No cracks were found in the deposits examined.

Corrosion Tests. These have been conducted under the same conditions as those in the first stage. We have, however, only used test coupons taken in the middle of the beads and of which the surface was left in the as-clad condition. No postwelding heat

Table 4—Stage 2 Deposit Composition and Ferrite Content

	Layers	Composition, % C	Mn	Si	Cr	Ni	Mo	N_2	Ferrite (magnetic permeability), %
ST 4	1	0.04	2.02	0.74	18.4	14.6	2.3	0.088	
	2	0.035	2.22	0.71	18.5	14.9	2.8	0.056	1.005
ST 5	1	0.04	1.61	0.58	16.3	12.6	1.95	0.028	
	2	0.025	2.04	0.75	18	14	2.2	0.03	1.006
ST 6	1	0.03	2.3	0.72	18.1	14.3	2.3	0.13	
	2	0.03	2.05	0.79	18.3	14.3	2.3	0.12	1.008
ST 7	1	0.035	2.1	0.77	18.3	14.2	2.1	0.19	
	2	0.025	2.05	0.84	18.3	14.5	2.5	0.14	1.006

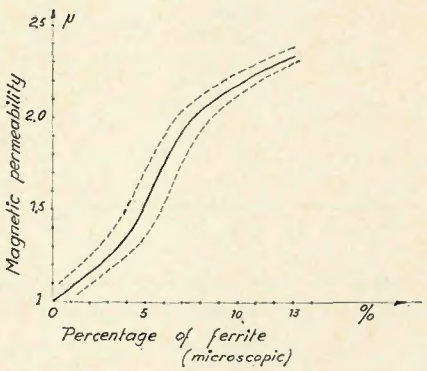

Fig. 2—Correlation curve as established in our laboratories for deposited metal between "magnetic permeability" readings with the Magnetoscope and microscopic counting. Dashed line curves—extreme values; solid line curve—average values

Table 5—Stage 2 Corrosion Test Results

Deposit	48 hr periods—loss in weight, g 1	2	3	4	5	Avg. loss, g	Surface, sq cm.	Corrosion rate, microns/ 48 hr	Local attack, microns
ST 4	0.0830	0.0615	0.0652	0.0761	0.0763	0.0664	30.2000	2.78	120
ST 5	0.0822	0.0540	0.0534	0.0626	0.1422	0.07888	30.1136	3.32	70
ST 6	0.0816	0.0494	0.0467	0.0553	0.1219	0.07098	30.0632	3.98	80
ST 7	0.0941	0.0561	0.0534	0.0645	0.0753	0.07087	29.2500	3.06	35

treatment has been applied. The complete results of the corrosion tests are reported in Table 5.

Observations. The four deposits tested are entirely satisfactory from all points of view. The principles on the basis of which these tests have been worked out are the same. The fact that their corrosion behavior is comparable, despite the differences in all round composition of the deposited metals, constitutes a confirmation of the validity of their application.

Stage 3

One principal aim of stage 3 was to confirm the good results obtained with one of the satisfactory deposits of stage 2. Another was to complete information regarding this result by corrosion tests on test coupons taken in the middle of the beads and on adjacent overlapping beads in considering two conditions of use—one as-welded and the other stress-relieved for 20 hr. at 550° C(1022° F).

Test ST 5 of stage 2 was selected for further tests because of its technological and chemical characteristics considered as a whole. This was designated as ST 8 because of a few composition adaptations which were made in comparison with ST 5. All the cladding conditions are identical to those used and described previously. The following coupons were sampled and subjected to magnetic permeability and corrosion tests: ST 8 MB—middle of the bead, as-welded condition no grinding; ST 8 MR—middle of the bead, stress relieved for 20 hr. at 550° C, no grinding; ST 8 CB—overlap, as-welded condition, no grinding; ST 8 CR—overlap, stress relieved for 20 hr. at 550° C, no grinding.

Chemical Composition and Magnetic Permeability. The chemical composition of the second layer of ST 8 metal deposit is given in Table 6. The magnetic permeabilities observed on each of the coupons submitted to corrosion are as follows: ST 8 MB—1.008; ST 8 MR—1.0095; ST 8 CB—1.012; ST 8 CR—1.008.

Metallographic Examinations and Corrosion tests. No crack or microcrack was found in the deposited metals.

The complete results from the corrosion tests are to be found in Table 7. The results obtained by the Staatsmijnen-Stami-Carbon laboratories are given between brackets. They are all expressed in micros per 48 hr.

Observations.

1. These tests confirm without exception the very good behavior previously observed in stage 2 tests.

2. There is no difference in corrosion results between the middle of the weld beads and the overlap area.

3. A stress-relieving treatment of 20 hr. at 550° C does not impair the corrosion resistance of the weld deposits considered. However, note again that specimen ST 8 is practically completely austenitic. More advanced investigations on alloys containing 0.5 to 1% ferrite have shown:

(a) A heat treatment at 500° C (932° F) for 20 hr. does not impair their corrosion resistance. The delta ferrite remains unchanged.

Table 6—Composition of Second Layer of ST 8 Metal Deposit, %

	C	Mn	Si	Cr	Ni	Mo	N_2
ST 8	0.024	1.80	0.81	18.4	15.8	2.40	0.03

Table 7—Stage 3 Corrosion Test Results

Coupons	48 hr periods—loss in weight, g 1	2	3	4	5	Avg. loss, g	Surface, sq cm.	Corrosion rate, microns/ 48 hr[a]	Local attack microns
ST 8 MD	0.0863	0.0589	0.0618	0.0598	0.0417	0.0617	35.840	2.18	10
	(3.12)	(2.20)	(2.16)	(2.23)	(2.40)	..	....	(2.42)	
ST 8 MR	0.0819	0.0627	0.0650	0.0677	0.0696	0.0693	35.390	2.48	55
	(3.47)	(2.48)	(2.29)	(2.43)	(2.44)	....	....	(2.62)	
ST 8 CB	0.0701	0.0481	0.0541	0.0529	0.0521	0.0581	36.4962	1.94	45
	(3.02)	(1.89)	(1.89)	(1.90)	(2.10)	....	....	(2.14)	
ST 8 CR	0.0787	0.0539	0.0584	0.0516	0.0606	0.0606	39.470	2.0	15
	(3.16)	(2.30)	(2.26)	(2.24)	(2.19)	....	....	(2.14)	

[a] Values in brackets indicate values found in the "Staatsmijnen" Stami-Carbon laboratories in microns/48 hr.

Table 8—Data for Steels with Required Dimension Delta Ferrite Pools

Steel Identification no.	Chemical composition, % C	Mn	Si	Ni	Cr	Mo	Cu	Ti	Ferrite content, % X-ray diffract.	Metallog	Condition
3522	0.027	1.1	0.5	11.2	17.2	2.5	0.05	0.08	1.5	1	Forged
				11.4	17.9	2.6					
3947	0.017	1.2	0.4	12.2	16.3	2.3	0.04	....	6	5	Cast
3948	0.027	0.7	0.4	11.6	16.8	2.6	0.04	....	5	4	Cast
				11.8	17	2.8					

(b) A heat treatment at 530° C for 15 hr. only slightly impairs the corrosion resistance, but the corrosion rates remain in the specified limits. The first signs of the transformation of delta ferrite to sigma phase are visible under the microscope.

(c) A heat treatment at 530° C for 15 hr. followed by a heat treatment at 600° C (1112° F) for 1 hr leads to a considerable increase of the corrosion rate which largely exceeds the permissible values. Microscopically the delta ferrite appears to be completely transformed to sigma phase.

It is of course important to take these observations into account for the choice of the correct "stress relieving" heat treatments into practice.

Conclusions on the Strip Cladding Development.

1. Satisfactory submerged-arc strip cladding consumables to deposit an alloy of the 316L low ferrite type have been developed.

2. This development has been essentially based on the metallurgical considerations which are further described in the second part of the present work. These considerations underline the influence of the following factors:

(a) Composition of the ferrite and austenitic phases in relation to the overall composition of the alloy and the ferrite contents.

(b) Rate and degree of transformation of the ferritic phase into sigma phase in relation to its composition and the welding thermal cycle.

(c) Influence of the structural changes on the corrosion rates of the alloys.

3. The proposed solution of the problem calls for the use of type AISI 309L strip for the first layer and type AISI 308L strip for the second layer. Each of these strips is employed with a specially conceived correcting flux which is peculiar to it.

4. The results obtained show that the proposed technique and consumables give a satisfactory cladding deposit without any restriction as regards to the severe quality requirements governing the use of stainless alloys in the field of urea synthesis.

5. The excellent results obtained from the laboratory tests have already been confirmed on the industrial scale.

Manual Arc Welding Electrode. It is finally to be noted that, besides the 316L-LF strip-flux combination, a special manual arc electrode has been developed. The metal deposited with this electrode is, from points of view of composition and corrosion resistance, similar to that which is deposited using strip cladding. It has an outstanding resistance to hot shortness and to cracking resulting from reheating by subsequent welds.

Industrial References. In the past two years many cylindrical tanks, hemispherical shells and tube plates have been successfully clad with the proposed new methods and consumables.

Part II—Detailed Metallurgical Investigations

The basic idea of the research work which is described below was to try to find an explanation for the accelerated corrosion rate of some of the above described 316L low ferrite type stainless steels in the as-welded condition.

It is generally admitted that this higher corrosion rate has something to do with the delta to sigma transformation which is believed to occur during welding.

The purpose was to study the distribution of the alloying elements Cr-Ni-Mo in the samples before and after the formation of sigma phase. This was done in order to observe eventual differences in this distribution, and to examine whether depleted or enriched zones—principally chromium depleted zones, as generally believed—are present around the transformed particles.

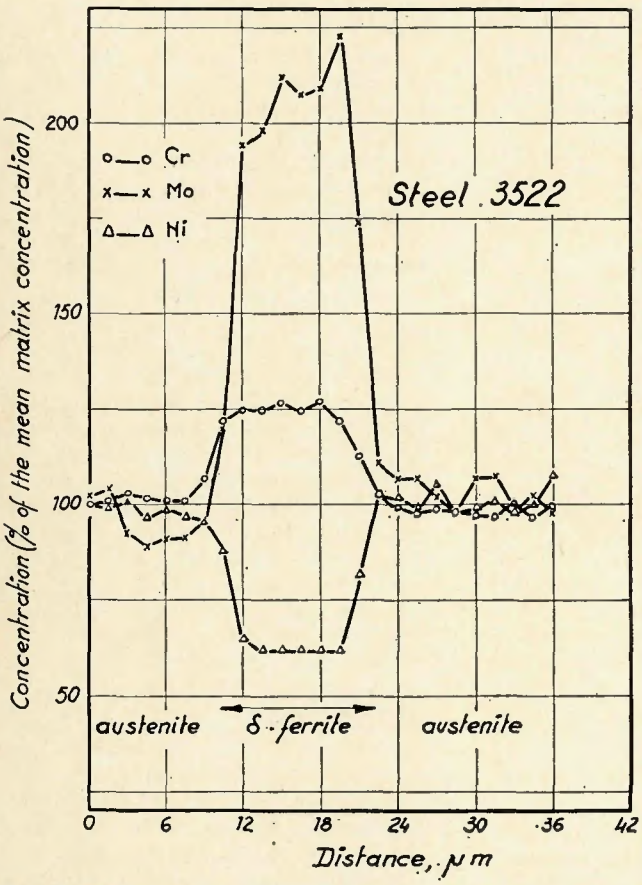

Fig. 3—Specimen no. 3522—distribution of Cr-Ni and Mo through austenitic matrix and delta ferrite pools as determined using microscan techniques

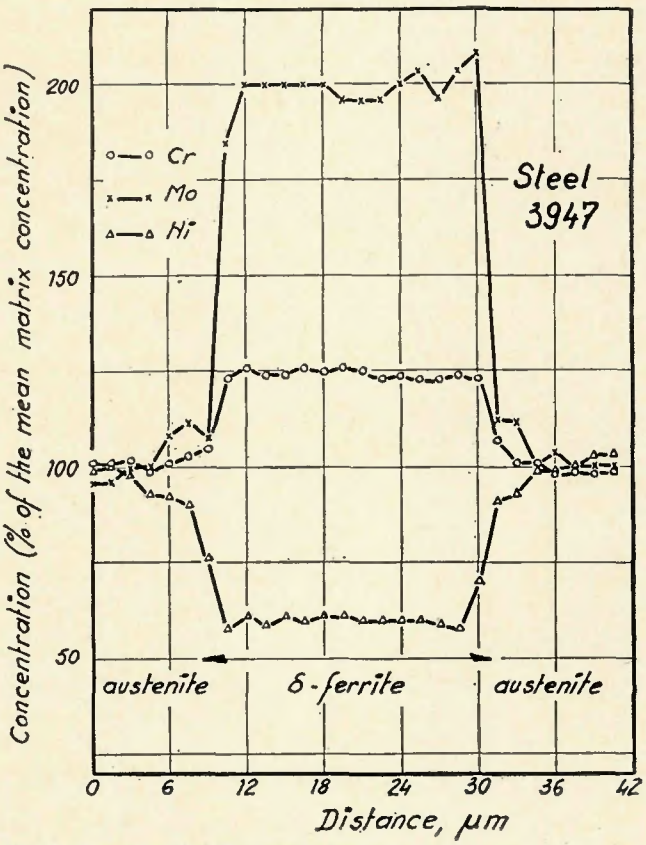

Fig. 4—Same as Fig. 3—specimen 3947

Specimens for Examination

The ideal approach would have been to examine directly samples of weld metal; however, we were limited as to the particle size of the ferrite and sigma pools, which have to be at least 3 microns in diameter for accurate electron probe microanalysis.

The very small dimensions of the ferrite pools in weld metal rendered their examination impossible. Therefore, the investigations have been performed on three samples of stainless steels in which the delta ferrite pools had the required dimensions. The composition of these steels, their ferrite level—determined by X-ray diffraction and metallographic estimation—and the condition in which they were considered, are given in Table 8.

Preliminary Microscopic Examinations

Using $FeCl_3$ + HCl as an etchant, a dendritic structure was clearly visible in steel n° 3947. This type of structure existed also in steel n° 3948 but was of course absent in steel n° 3522.

Microscan Investigations

The microscan investigations have been performed, using a Cambridge microscan apparatus, on small specimens which have been cut out by electroerosion. The dimensions of the specimens were $^1/_4$ in. in diameter and $^1/_4$ in. long.

Variations of Composition Across the Austenite Dendrites

The alloying elements Cr, Ni and Mo have been studied. In order to record the distribution curves of these alloying elements across the dendrite axes, an ultra slow scanning technique was used; instead of using a single displacement of the spot along the scanning line, use was made of a transversal scanning on a 50 micron wide zone along this line.

This method made it possible to eliminate variations in concentration due to the presence of delta ferrite pools, as each point of the chart gives the mean analysis of a 50 micron wide zone. The longitudinal scanning line is directed across the dendrite axes while the transveral scanning is parallel to them.

Steel 3947 with its clearly visible dendritic structure is the only one in which a significant enrichment of Cr, Ni and Mo was found in the dendrite axis. This particular distribution was most clearly visible on the Mo concentration curves. However, it was not important enough to be investigated more thoroughly.

Distribution of Alloying Elements Between Austenite and Ferrite

The concentrations of Cr, Ni and Mo in the austenitic matrix and in the delta ferrite pools were determined using spot analysis. The most important results are summarized in Fig. 3 to 5, respectively for the steels n° 3522, 3947 and 3948. The vertical scale indicates the relative concentrations of Cr, Ni and Mo in a given delta ferrite pool, in % of the mean concentration of these elements in the matrix.

Independently of the ferrite content of the considered alloys, it has been observed that in the delta ferrite phase we have:

1. Enrichment of Cr to about 125% of base.
2. Enrichment of Mo to approximately 200%, of base.
3. Impoverishment of Ni to about 60%, of base.

Considering different delta ferrite particles in the same specimen, it was found that Cr and Ni concentrations were very reproducible but that the Mo concentrations showed larger variations. Since it is known that Mo promotes the delta to sigma transformation, it can be assumed that the most Mo rich ferrite pools of a given alloy are the first affected when this type of transformation occurs.

Finally, an attempt was made to determine the relative concentrations of silicon in the austenite and in the ferrite. However, because of both the low silicon level of the alloys and the weak response of that element, it was impossible to find significant differences.

The Delta Ferrite to Sigma Transformation

This type of transformation has been studied by submitting several samples of the steel n° 3947 to different heat treatments. The aim was to determine whether it was possible to find differences in concentration of Cr, Mo and Ni between the original delta ferrite and the subsequently formed sigma phase and/or to find Cr

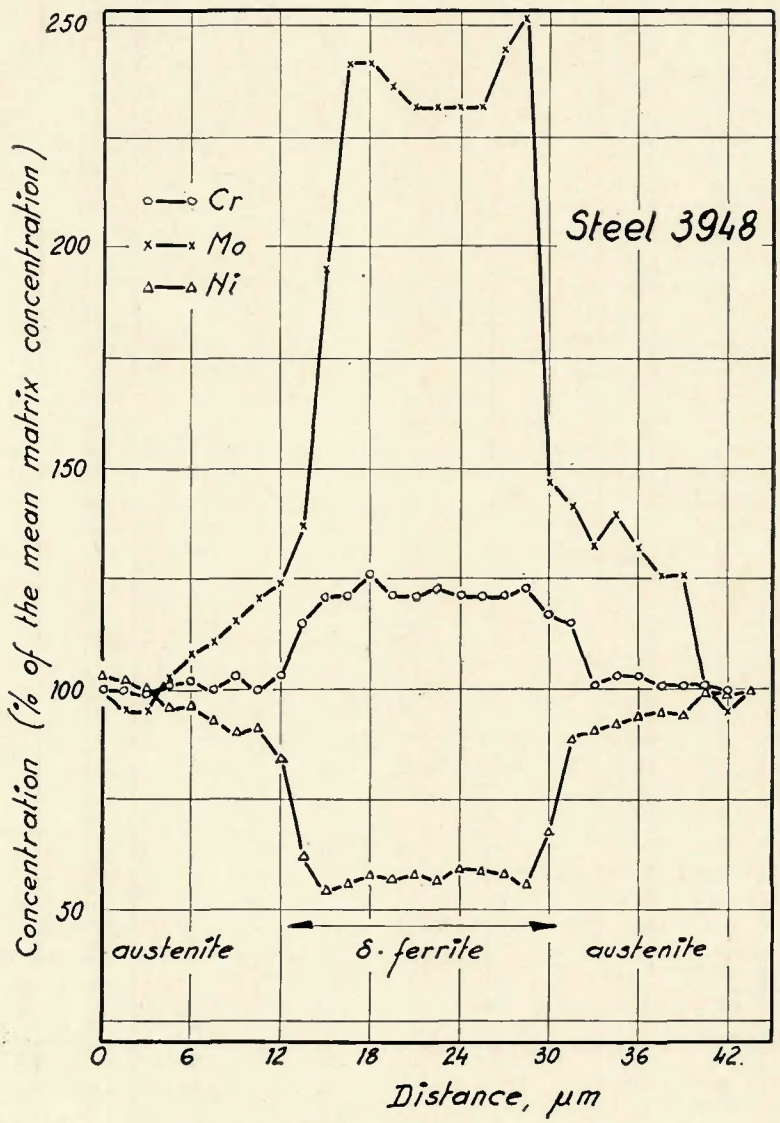

Fig. 5—Same as Figs. 3 and 4—specimen 3948

Fig. 6—Specimen 3947—untransformed delta ferrite. Electrolytic etch. ×500 (reduced 42% on reproduction)

Fig. 7—Specimen 3947—heat treated 2 min at 850 C. First stage of delta ferrite to sigma phase transformation. Electrolytic etch. ×500 (reduced 42% on reproduction)

Fig. 8—Specimen 3947—heat treated at 2 min at 850° C. Further view of first stage of delta ferrite to sigma phase transformation. Electrolytic etch. ×500 (reduced 42% on reproduction)

depleted zones around the ferrite pools which are transformed to sigma phase.

In order to avoid interferences with diffusion effects, the sigmatisation of the samples has been performed as follows:

1. The specimens have small dimensions—$^1/_4$ in. in diameter and $^1/_4$ in. in length.
2. The thermal heat treatment have been given at 850° C, which represents a very high transformation rate, for different times—1, 2, 3, 4, 5, 10, 20 and 30 minutes.
3. The specimens were heated very rapidly by putting them in the oven at 850° C.
4. The specimens were quenched in water at room temperature after heat treatment.

Results of Metallographic Examinations

In samples which were treated for 1 or 2 minutes, we found some unattacked ferrite pools, other particles which were attacked at the borders, and other ones which were totally etched, and thus totally transformed. After 4 or 5 minutes of thermal treatment the transformation proved to be complete. This is illustrated in Figs. 6–9.

Etchants which normally do not attack the delta ferrite and the sigma phase which is formed at lower temperatures,[4] proved to be very efficient in the present case. Using those etchants on the heat-treated and sigmatised specimens, all the transformed ferrite pools appeared to be very deeply etched. This undoubtedly is some indication of an increased corrosion susceptibility of the steel.

It is the opinion of some authors[5] that the phase which is formed is a carbide-austenite mixture rather than a sigma-austenite mixture. Since in the present case, the size of the individual particles of those components is very small, it has not been possible to determine their exact nature using diffraction techniques. This means that there is not a valid method available to determine whether those particles are carbides or not.

Fig. 9—Specimen 3947—heat treated 5 min at 850 C. Final stage of delta ferrite to sigma phase transformation. Electrolytic etch. ×500 (reduced 42% on reproduction)

However, our statement that the newly formed phase is actually sigma phase can be supported by the following considerations:

1. The chemical composition which we have found for the ferrite phase, the rate of transformation and the kinetics of transformation at 850° C which we have observed are all in favor of the formation of sigma phase in accordance with the well known "chrome-iron" equilibrium diagrams.
2. Carbide precipitation does preferentially occur in grain bounderies, especially on the interfaces of austenite and ferrite. Even considering high carbon stainless steels subjected to long duration heat treatments at high temperature, this location of carbide precipitates remains the same.

Since the alloys that were considered have very low carbon contents (less than 0.03%) and also considering the fact that the whole volume of the ferrite pools is completely transformed after very short times at 850° C, and although the transformation also starts at the delta-gamma interfaces, it must be admitted that the newly formed phase is sigma phase.

Results of Electron Microprobe Analysis

In order to determine the compositions of the transformed ferrite pools and of the surrounding austenite, it appeared to be impossible to examine etched specimens using the electron microprobe technique. The deep corrosion of the sigma phase resulted in very important disturbances of the results.

As a consequence the electron microprobe examinations have been conducted using the following method:

1. After a first etching, the sigma phase particles are localized by means of microhardness indentations.
2. The specimens are then repolished in order to remove the surface layer, however, without complete removing of the hardness indentations.
3. The microprobe investigations are finally performed on the marked zones of the unetched specimens.

This method proved to be successful and distribution curves for Cr, Ni and Mo; these curves were exactly the same as in the case of the original delta ferrite. In no case was a chromium-depleted zone found in the neighborhood of the transformed particles.

Since the transformation, at 850° C, proceeds very rapidly, and also since the diffusion of elements, such as C, Fe, Cr, proceeds very slowly at this temperature, one must admit that the delta to sigma transformation is under these circumstances a type of "in site" transformation occurring without long-range diffusion.

As a result a mixture of finely dispersed sigma and gamma particles is formed in the sites of the original ferrite. The diameter of the spot which is irradiated using electron microprobe analysis is of the order of 2 microns in diameter. This is large compared with the dimensions of the individual sigma and gamma particles, so that the distribution curves obtained for Cr, Ni and Mo in the transformed areas represent the average composition of the sigma-gamma mixture which, taking in account the absence of diffusion, is the same as in the original ferrite, as shown in Figs. 3–5.

From point of view of diffusion, it

further cannot be easily admitted that we should have some important chromium depleted zones around the sigma pools. As already mentioned, the transformation rate appears to be too high.

By lowering the heat treatment temperature in order to decrease the transformation rate, it would of course be possible to have long distance diffusion, but this would also result in an homogenization of the austenite around the sigma phase pools. This means that we have not, in fact, a valid method to prove the existence of very small chromium-depleted zones.

Conclusions

1. At 850° C the transformation of ferrite to sigma phase occurs very rapidly in the alloys studied. Taking in account both the slow cooling rates during strip welding and the fact that the ferrite pools have smaller dimensions in a weld metal than in the cast or forged steels, it is possible to justify the presence of sigma phase in as deposited weld metal. In order to avoid this type of transformation which is detrimental for the corrosion resistance of the alloys, the welding consumables must be specially designed.

2. The rapid transformation of ferrite to a sigma phase in these low ferrite alloys is characterized by the following particularities:

(a) The transformation occurs without long distance diffusion.

(b) It starts at the ferrite-austenite interfaces and progresses very rapidly. The ferrite pools which are first transformed are those where the Mo content is believed to be the highest.

(c) The so called "sigma-phase" is in fact a mixture of very finely dispersed sigma and gamma particles. This means that the specific contact surface between sigma and gamma particles is very high.

(d) The composition of this mixture proved to be the same as that of the original ferrite.

(e) In the present case it is not believed that carbide precipitation interferes with the sigma transformation.

(b) It has not been possible to find chromium depleted zones around the sigma phase pools. If such zones exist, they must be of very small dimensions.

3. The sigma-gamma mixture which is formed in the sites of the original ferrite proved to be very corrosion sensitive. All the etchants are likely to produce very pronounced corrosion effects on those areas. As a result, the higher corrosion rates observed on sigmatised 316L low ferrite alloys can be explained on ground of the following mechanism:

(a) The corrosion does not seem to occur as a result of electrochemical potential differences between the sigma pools on one hand and the austenitic matrix or a chromium depleted austenite around the sigma pools on the other hand.

(b) The corrosion seems to occur as a result of electrochemical potential differences between the sigma and the gamma particles in the transformed areas. The higher the transformation rate of ferrite to sigma, the finer the sigma and gamma particles, the higher the specific surfaces of these particles and the higher the corrosion rate of the alloy.

References

1. "Stainless Steel Strip Cladding on Carbon-Ferritic Base Metals," final report, EURATOM—USAEC Contract n° 008-63-12 TEEB.
2. Espy, R. H., "Effect of Composition on the Corrosion Resistance of as Welded 316 L Stainless Steel Weld Deposits," paper presented at the Midwest Welding Conference, Chicago, January 1964.
3. Hall, E. D., and S. H. Algie, "The Sigma Phase," Journal of the Institute of Metals, n°. 4, April 1966.
4. Mommens, Marc, "Metallografische studie van de sigma fase en de delta ferriet fase in Cr-Mn stalen," thesis, 1968, Statts Universiteit Gent.
5. Strickler, R., and Vinckier, A., "La morphologie des carbures de chrome et son influence sur la corrosion inergranulaire d'un acier inoxydable 18/8," Mémoires Scientifiques de la Revue de Métallurgie LX, n° 7-8, 1963.

USSR Welding Research News

(*Continued from page* 32-s)

• Esibyan, E. M. and Danchenko, M. E.: AVPR-1 equipment for air-plasm-cutting of metals (69-71).

Svarochnoe, Proizvodstvo No. 2

• Lebedev, B. D.: The problem of carbon equivalent (1-2).
• Nikolaev, G. A. and Kiselev, A. I.: Function of the soft in brazed joints (3-4).
(Feb. 1969)
• Pridantsev, M. V. et al.: Heat-resistant properties of welded joints in austentic chromium-manganese steel with higher aluminum and carbon content (4-5).
• Bakshi, O. A. et al.: Fatigue strength of welded joints in 17 GS steel (6-7).
• Steklov, O. I. and Padaev, A. S.: Effect of nonuniformity of plastic deformation on corrosion cracking of welded joints (7-9).
• Donchenko, E. A. et al.: Effect of heat treatment on the redistribution of chromium, manganese and silicon in the overlay zone (9-11).
• Kuz'min, G. S. and Lazarson, E. V.: Behavior of oxygen, hydrogen and nitrogen in the gas-shielded-arc welding of nickel (11-13).
• Livshits, M. G. et al.: Strength of fillet welds (13-14).
• Lepciko I. P.: Influence of equipment load factor on production cost of welding (15-16).
• Polnarev, A.M.: Economic efficiency of centralized CO_2 supply system in the welding shop (16-18).
• Postovalov, Yu, I. et al.: Electroslag welding of circumferential joints at the Urals Machine Works (18-21).
• Rapaport, E. A.: Condensor welding of springs with contacts (21-22).
• Tsygan, B. G. et al.: Characteristics and technology of applying corrosion resistant overlays with vibrating electrodes (22-25.)
• Molchanov, V. D. and Chernykh, N. P.: Effect of hydrogen on the properties of welded joints in high pressure vessels (25-28).
• Astaf'ev, A. S.: Determination of some mechanical properties in the heat-affected zone (28-29).
• Kuznetsov, B. A.: The problem of metal deformation in the HAZ in the welding of type 18-8 steel (29-30).
• Kiselev, S. N. et al.: Residual stresses in welded joints in aluminum pipes (30-31).
• Pastukh, M. N.: and Borovskikh, S. N.: Manual argon arc welding of CAC1 (A1-28Si-6 Ni) alloy (31-32).
• Nazarov, G. V. et al.: Control of contact micro welding, using initial resistance (33-35).
• Volovik, A. Ya. and Kiselev, E. D.: Low-temperature resistance of CO_2-welded joints (35-36).
• Tkachev, V. N. and Kagan, A. L.: Longer service life for working parts of earth-moving equipment by resistance-welded alloy strips (37-38).
• Patskevich, I. R. et al.: Vibro-arc application of bronze overlap on steel rods and pistons (38-39).
• Shapiro, I. S. et al.:Plasma arc cutting of thin gage metal (40).